horticulturae

MDPI

Article

Efficient Editing of *SoCSLD2* by CRISPR/Cas9 Affects Morphogenesis of Root Hair in Spinach

Yingping Cao [1,2,†], Yue Xu [2,†], Yue Zhang [1,3], Heng Zhang [1], Zhi Qin [1], Chen Bai [1,2], Hailing Zhang [4], Dongmei Ma [5], Quanhua Wang [1], Chunxiang Fu [2], Meihong Sun [1,*] and Shaojun Dai [1,*]

1 Development Center of Plant Germplasm Resources, College of Life Sciences, Shanghai Normal University, Shanghai 200234, China
2 Shandong Technology Innovation Center of Synthetic Biology, Shandong Provincial Key Laboratory of Energy Genetics and CAS Key Laboratory of Biofuels, Qingdao Institute of Bioenergy and Bioprocess Technology, Chinese Academy of Sciences, Qingdao 266000, China
3 Key Laboratory of Saline-Alkali Vegetation Ecology Restoration, Ministry of Education, College of Life Sciences, Northeast Forestry University, Harbin 150040, China
4 Grass and Science Institute of Heilongjiang Academy of Agricultural Sciences, Harbin 150086, China
5 Breeding Base for State Key Laboratory of Land Degradation and Ecological Restoration in Northwestern, Key Laboratory of Restoration and Reconstruction of Degraded Ecosystems in Northwestern China of Ministry of Education, School of Ecology and Environment, Ningxia University, Yinchuan 750021, China
* Correspondence: sunmeihong@shnu.edu.cn (M.S.); daishaojun@shnu.edu.cn (S.D.)
† These authors contributed equally to this work.

Abstract: CRISPR/Cas9 is a valuable tool and has been extensively employed to perform gene editing in plants. However, CRISPR/Cas9 has not been successfully used in spinach, an important leafy vegetable crop. Here, we established a CRISPR/Cas9-based gene-editing system for spinach hairy roots and edited two cellulose synthase-like D (*CSLD*) genes (*SoCSLD2* and *SoCSLD3*) that were involved in root-hair formation of spinach hairy roots. Four mutation types (i.e., replacement, insertion, deletion, and combined mutations) were observed, among which the replacement accounted for the vast majority (about 64.1%). Mutation rate differed largely among different targets. Seven homozygous/bi-allelic and eight heterozygous/chimeric mutants of *SoCSLD2* were obtained from 15 independent transgenic hairy root lines. All of the seven homozygous/bi-allelic mutant lines displayed bulking and short root hairs, which resembled the characteristics of *Arabidopsis atcsld2* mutants. The transcriptomic analysis further revealed that multiple gene expressions for cell-wall modulation and membrane trafficking were disturbed, which might result in the inhibition of root hair growth in *socsld2* mutants. This indicates that *SoCSLD2* was successfully knocked out in spinach root hairs using the CRISPR/Cas9-based gene editing system.

Keywords: CRISPR/Cas9; cellulose synthase-like D (*CSLD*) gene; spinach; hairy root; root hair; transcriptomic analysis

Citation: Cao, Y.; Xu, Y.; Zhang, Y.; Zhang, H.; Qin, Z.; Bai, C.; Zhang, H.; Ma, D.; Wang, Q.; Fu, C.; et al. Efficient Editing of *SoCSLD2* by CRISPR/Cas9 Affects Morphogenesis of Root Hair in Spinach. *Horticulturae* **2022**, *8*, 735. https://doi.org/10.3390/horticulturae8080735

Received: 17 June 2022
Accepted: 12 August 2022
Published: 16 August 2022

1. Introduction

Spinach is an important nutritious green leafy vegetable, which is rich in carotenoids, folate, vitamin C, as well as calcium and other irons [1]. We have published the genome sequence of a Chinese inbred spinach cultivar Sp75 (*Spinacia oleracea*, 2 *n* = 12) [1,2] and provided a preliminary *Agrobacterium rhizogenes*-mediated transformation system of spinach [3]. We also have cultured new spinach varieties with higher stress (e.g., heat, salinity, and disease) tolerance using traditional and molecular breeding strategies [4]. The specific heat-responsive signaling and metabolic mechanisms in heat-tolerant spinach variety Sp75 and heat-sensitive variety Sp73 have been reported using proteomics and phosphoproteomics approaches [5,6]. However, due to lack of a highly efficient gene-editing system, the gene functions have not been proved by molecular genetics, although numbers of genes/proteins have been identified and are proposed to be involved in transcription,

calcium signaling, ROS homeostasis, endomembrane trafficking, and cross-membrane transport in spinach [5–7]. Therefore, establishment of a gene-editing system is critical for the investigation of molecular mechanisms in spinach development and stress responses.

The clustered regularly interspaced short palindromic repeat (CRISPR)-associated protein (Cas9) system is firstly discovered to function as a component of the immune system from the bacterium *Streptococcus thermophilus* [8]. In this system, an engineered single-guide RNA (sgRNA) could form a complex with Cas9 nuclease and guide the complex to target DNA sequence, which can pair with the former 20 bases of sgRNA, followed by an "NGG" sequence for the binding and cleavage of SpCas9 nuclease [9–12]. Homologous recombination (HR) and non-homologous end-joining (NHEJ) are promoted in the higher organisms by the site-specific double-strand breaks generated by Cas9 nuclease, which resulted in targeted mutagenesis. In recent years, the type II CRISPR-Cas9 system through *Agrobacterium tumefaciens* transformation has become a powerful tool for investigating plant gene function and crop molecular breeding, but its applications are limited for lack of mature transformation platforms for some plants [13,14]. Fortunately, *A. rhizogenes*-mediated transformation system succeeds more readily in plants because it induces the production of hairy roots rather than aiming at germline transmission. It would be a satisfactory system after the regeneration from hairy roots is figured out in the coming future [15].

Root hairs have important roles in uptake of water and nutrients and also affect the surface area between plants and soil microbes [16]. Root hairs are tubular outgrowths of specialized root epidermal cells, which need rapid cell-wall assembly in the tips. The deficient and/or disrupted cell-wall components lead to root hairs that are deformed and even ruptured [17]. Cellulose, hemicellulose, and pectin are the main components of plant cell walls [18]. A number of genes are involved in regulation of these component metabolism for cell-wall modulation upon hair tip growth. Cellulose synthase (CESA) proteins are responsible for the synthesis of cellulose, while CELLULOSE SYNTHASE-LIKE (CSL) proteins are involved in the synthesis of hemicellulose [19,20]. Arabidopsis *CSL* gene family contains 30 genes, which are divided into six groups (i.e., *CSLA*, *CSLB*, *CSLC*, *CSLD*, *CSLE*, and *CSLG*) [21]. Among them, *CSLD* gene plays critical roles in the cell-wall development of root hairs [22].

Arabidopsis has six *AtCSLDs*, and *AtCSLD2* and *AtCSLD3* are required for normal root hair growth [17,22,23]. *AtCSLD3* is involved in the biosynthesis of β-glucan-containing polysaccharides in cell wall for root-hair elongation [24,25]. More AtCSLD2 is required during the late stage of hair development than AtCSLD3 [22]. The *atcsld2* mutant exhibits abnormal root hair and many root hairs bulging and rupturing late during the root development process [22]. The root-hair phenotype analyses of *atcsld2* single mutants, the *atcsld3* single mutants, double homozygote (*atcsld2/atcsld2 atcsld3/atcsld3*), and double heterozygote (*AtCSLD2 atcsld2*/*AtCSLD3 atcsld3*) indicates that *AtCSLD2* and *AtCSLD3* regulate the root-hair growth in a dosage-dependent manner [26]. Moreover, *AtCSLD3* may exhibit more prominent effect than *AtCSLD2*, although *AtCSLD2* and *AtCSLD3* have redundant function in root-hair development [26]. The functions of *CSLDs* have been reported in various crops and trees [26–30]. For example, cotton *GhCSLD3*, the ortholog gene of *AtCSLD3*, partially rescues the growth defect of *atcesa6* mutant [26,27]. The primary wall cellulose production, cell elongation, cell wall integrity, and dry weight are all increased in *GhCSLD3* overexpression seedings in the background of *atcesa6* mutant [27]. Besides, *Populus trichocarpa* genome contains ten *CSLD* genes (*PtrCSLD1-10*) [28]. Complementation of *atcsld3* mutant with *PtrCSLD1-10* reveals that only *PtrCSLD5* could rescue the root-hair defect phenotype of *atcsld3* mutants, which is supposed to be the functional ortholog of *AtCSLD3* in root-hair formation [28]. Interestingly, in another poplar species *Populus deltoids*, *PdCSLD5* and *PdCSLD6* can rescue the root hair defects and cellulose contents in *atcsld3* mutants [23]. In addition, a short or variable root hair phenotype is observed in several allelic mutant lines of *LjCSLD1* in crowtoe (*Lotus japonicus*) [29]. The complementation experiments by expressing *LjCSLD1*, *AtCSLD2*, and *AtCSLD3* in the background of *Ljcsld1-1*, *Ljcsld1-2*, and

Ljcsld1-6 mutants indicates that *LjCSLD1* functions as a homozygous of *AtCSLD2* and *AtCSLD3* [29]. Moreover, *Ljcsld1-1* and *Ljcsld1-6* mutants show an increased cell-wall thickness. The heterozygous *LjCSLD1/Ljcsld1-1* exhibits an intermediate root hair length of wild-type, which indicates that *Ljcsld1-1* has a semi-dominant effect on the root hair growth [29]. Together, this indicates that the members of *CSLDs* in various plants are relative conserved and probably play crucial roles during cell-wall formation in a dosage-dependent manner. However, the function of *SoCSLDs* in spinach cell-wall development is still unclear.

Establishment of a high-efficiency gene-editing method in spinach using the optimized CRISPR/Cas9-based gene-editing system and *A. rhizogenes*-mediated hairy root platform was pivotal for performing the molecular genetics investigation. Because of the aforementioned vital roles of *CSLD* genes in regulating root-hair growth and observable root hairless phenotype of *atcsld2/3* mutants, spinach *SoCSLD2* and *SpCSLD3* were chosen as the target genes for gene editing in this study. The abnormal root hairs were observed in homozygous/biallelic mutant lines of *SoCSLD2*, and the transcriptome analysis revealed that the cell-wall-related signaling and metabolic processes were disturbed in *socsld2* mutants, which indicated that the CRISPR/Cas9-based gene editing had been successfully applied in hairy roots of spinach.

2. Materials and Methods

2.1. Plant Materials, Growth, and Culture Conditions

Chinese inbred spinach variety Sp75 was used in this study [1]. The seeds were surface-sanitized with 75% ethyl alcohol and 5% sodium hypochlorite [2]. All the sterile seeds were germinated on solid 1/2 MS basal medium containing 30 g/L sucrose and 10 g/L agar and cultured under 26 °C and 16 h light/8 h dark. The explants from leaves were used to induce hairy roots. The different tissues and organs from two-month-old seedlings were used for qRT-PCR analyses. Two-month-old hairy roots from normal wild-type (WT) and homozygous *socsld2* mutant (line 3) were collected for transcriptomic analysis.

2.2. Bioinformation Analysis of CSLD Protein Sequence

The five *SoCSLDs* gene sequences were achieved by BLAST using the *AtCSLD3* gene as a query sequence on the website (http://www.spinachbase.org/, accessed on 26 May 2021). Multiple alignment analysis of the full-length protein sequences was performed by Clustal X program. The phylogenetic tree was constructed with MEGA 3.1 program using the neighbor-joining (NJ) method with 1000 bootstrap replicates. The pI and molecular weight (MW) of SoCSLD2 and SoCSLD3 were predicted on the website (https://web.expasy.org/compute_pi/, accessed on 26 May 2021). The conserved domains of SoCSLD2 and SoCSLD3 were analyzed online by the Conserved Domain Database (CDD) of NCBI (https://www.ncbi.nlm.nih.gov/cdd, accessed on 26 May 2021).

2.3. Quantitative Real-Time PCR

Total RNAs were extracted from stem, leaf, flower, stipe, root, and hairy root using Trizol reagent (Invitrogen Corporation, Waltham, MA, USA). RT-PCR was carried out using 500 ng of total RNA with PrimeScript™ RT reagent Kit with gDNA Eraser (TaKaRa) following the manufacturer's protocol. Gene expression was assayed using an Rroche LightCycler480 real-time PCR System. The expression of *actin* gene (*Spo23599*) was used as an internal control. The primers used to amplify transcripts were listed in Supplementary Table S8, and qPCR was performed according to the manufacturer's protocol of *TransStart* Green qPCR Super Mix (AQ101). The PCR procedure included: one cycle of 95 °C for 2 min, 30 cycles of 95 °C for 15 s, 60 °C for 15 s, and 72 °C for 30 s. Three biological replicates were performed. Students *t*-test ($p < 0.01$) were used for statistical analysis.

2.4. Target Sites Design and Vector Construction

The specific sequences of *SoCSLD2* and *SoCSLD3* were amplified by two pairs of primers (Supplementary Table S8), respectively. Three target sites were selected for each

gene according to Ma et al. [10] (Supplementary Figure S1a,b). Briefly, the 20 bp sequence before the NGG region should have appropriate GC content (≥30%), avoid four consecutive T nucleotides, and exclude the target candidates that form the hairpins of longer than 6 bp with sgRNA sequence. The tRNA–gRNA cassette strategies were used [30]. *Cas9* was driven by the CaMV *35S* promoter. Target sequences separated by tRNA and followed by one gRNA were driven by Arabidopsis *U3b* promoter. *Bar* gene driven by CaMV *35S* promoter was used as a selective marker (Supplementary Figure S1c). We constructed a modified pYLCRISPR/Cas9 35s-B (GenBank accession number: AI133729.1) vector. The segment of two *Bsa I* cutting sites and CCDB in the vector was replaced with the sequence containing an *AtU3b* snRNA promoter, two new *Bsa I* cutting sites, and a sgRNA sequence. *AtU3b* snRNA promoter was amplified from pYLsgRNA–*AtU3b* (GenBank accession number: KR029097.1) (Supplementary Figure S1d). The tRNA–gRNA cassette was linked to the constructed vector according to the methods of Ma et al. [10] and Xie et al. [30]. The fragments containing tRNA and/or sgRNA sequence were amplified from pGTR vector (Beijing Genomics Institute, Beijing, China) using the primers listed in Supplementary Table S8. The mixed fragments and the modified pYLCRISPR/Cas9 35s-B vector were digested by *Bsa I* and linked by T4 ligase in one step [8,23]. The CRISPR/Cas9 vector for *SoCSLD2* and *SoCSLD3* containing three target sequences and tRNA–gRNA expression cassette were transferred into *A. rhizogenes* strain LBA9402 for subsequent experiment.

2.5. Induction and Identification of Transgenic Hairy Roots of Spinach

A. rhizogenes strain LBA9402 carrying the CRISPR/Cas9 vector for *SoCSLD2* and *SoCSLD3* was used for the gene transfer experiment. The *Agrobacterium* strain was cultured by shaking in liquid LB containing 50 mg/L kanamycin and 20 mg/L rifampicin at 28 °C and under 200 rpm. The OD_{600} of 0.6–0.8 was the proper concentration for inoculation. The bacterial liquids were collected and re-suspended to OD_{600} of 0.2 using liquid MS medium containing 100 µM acetosyringone. The leaf discs (~0.5 cm × 0.5 cm) taken from the 30-day-old aseptic seedlings were submerged in *A. rhizogenes* suspension for 10 min and then co-cultured for two days in darkness. The discs were sub-cultured in a selection medium (SH base medium containing 1 mg/L phosphinothricin and 300 mg/L timentin). Hairy roots (2 cm in length) were cut from the discs and sub-cultured in the selection medium for further identification.

The genomic DNA of the putatively transformed plants was extracted using CTAB method. In order to identify the transgenic hairy root lines, PCR analyses were performed to detect the presence of *bar*, *Cas9*, and *rol B* genes using primers in Table S8.

2.6. Mutation Type Analysis

Fragments containing the target sites were amplified using the primer in Supplementary Table S8. The PCR products were sequenced to detect mutagenesis. The PCR sequencing results with mixed peaks and sequence changes in the target sites of *SoCSLD2* and *SoCSLD3* were included in Supplementary Figure S2. The PCR products with mixed peaks and/or sequence changes were purified with DNA Purification Kit and ligated in the pMD19-T easy vector. The ligated products were transformed into *Escherichia coli* strain Top10, and three positive clones of each transgenic line were sequenced to analyze their specific mutation types (Supplementary Sequencing Data). The protein sequence alignment analysis of WT and knockout lines of *SoCSLD2* are provided in Supplementary Figure S3.

2.7. Phenotype Observation

The phenotype of root hairs was observed under a microscope OLYMPUS SZX16 (Olympus Corporation, Tokyo, Japan). The length and density of root hairs were measured from three lines of mutants and normal hairy roots, respectively (n = 8).

2.8. Off-Target Analysis

The potential off-target sites were predicted according to the method of Li [24]. Spinach genome was downloaded from website (http://www.spinachbase.org/, accessed on 7 May 2021). The putative off-target locus was blasted among the whole genome of spinach. The sites containing no more than 3 bp mismatches in the 20 bp target sequence were taken as potential off-target sites (Supplementary Table S2). The sequences containing the potential off-target sites were amplified by PCR using gene-specific primers (Supplementary Table S8). The PCR products were sequenced to verify the occurrence of mutation (Supplementary Sequencing Data).

2.9. Transcriptome Sequencing of Root Hairs

Total RNA was extracted from hairy root of normal wild type (control) and *socsld2* mutants using the mirVana miRNA Isolation Kit (Ambion, Austin, TX, USA). The samples with RNA Integrity Number (RIN) $\geq$ 7 were subjected to the subsequent analysis. The cDNA library was constructed using TruSeq Stranded mRNA LTSample Prep Kit (Illumina, San Diego, CA, USA), and the libraries were sequenced on the Illumina sequencing platform (HiSeqTM 2500 or Illumina HiSeq X Ten) according to the method of Xu et al. [1]; 125 bp/150 bp paired-end reads were generated. The transcriptome de novo assembly was carried out using Trinity (http://trinityrnaseq.sourceforge.net, accessed on 27 April 2021). The clean reads were mapped to spinach reference genome using hisat2.

Fragments per kilobase of transcript per million (FPKM) of each gene and read counts value of each transcript (protein_coding) were calculated using bowtie2 and eXpress, respectively. The analysis of differential expression gene (DEG) among samples was performed using the DESeq (2012) R package. A p value < 0.05 and Fold Change > 2 (or <0.5) were applied to evaluate the difference significance. Hierarchical cluster of DEGs was performed to explore transcripts expression pattern. The detailed annotation information of DEGs is listed in Supplemental Table S3. GO and KEGG pathway enrichment of DEGs were performed using R based on the hypergeometric distribution. A network of enriched terms of GO biological processes and KEGG pathways across the DEG lists of the two clusters was visualized using Cytoscape 3.7.1 software. Each node represents an enriched term. The term genes next to the nodes are shown in Supplemental Table S4.

Heatmap was plotted using an OmicShare tool (http://www.omicshare.com/tools/, accessed on 8 May 2021). The KEGG pathway, as well as GO biological processes and cellular component enrichment analyses, were conducted using the Metascape analysis (http://metascape.org/, accessed on 8 May 2021). Terms with a p-value < 0.01, a minimum count of 3, and an enrichment factor (the ratio between the observed counts and the counts expected by chance) >1.5 were collected and grouped into clusters on the bases of their membership similarities.

Protein–protein interaction between DEG encoding proteins were predicted by the online tool STRING 10 (http://string-db.org/, accessed on 10 May 2021) with the minimum required interaction score set as >0.4. All other parameters were set as defaults, and all active prediction methods were used. The network was visualized using Cytoscape 3.7.1 software (http://www.cytoscape.org/, accessed on 10 May 2021). All the identification (ID) input for the interaction network analyses were protein homologs in *A. thaliana*, which were found by sequence BLASTing in the TAIR database. Proteins (nodes) were shown as bubbles whose color gradient from light blue to dark green according to the node degree distribution. The related interactions (edges) between proteins were shown as gray lines, whose width represented the strength of interaction score. The function categories were represented by different colors of bubbles in network and columns.

3. Results

3.1. SoCSLD2 and SoCSLD3 Were Strongly Expressed in Roots and Hairy Roots

Five spinach genes, *SoCSLD1* (*Spo16352*), *SoCSLD2* (*Spo23361*), *SoCSLD3* (*Spo10340*), *SoCSLD4* (*Spo12722*), and *SoCSLD5* (*Spo16366*), were predicted from the spinach (*S. oleracea*)

genome based on their similarity to the Arabidopsis *AtCSLD3* gene [24]. Phylogenetic analysis of the spinach and Arabidopsis AtCSLDs indicated that the five spinach genes were clustered with different AtCSLD genes. Among them, SoCSLD2 and SoCSLD3 were clustered with AtCSLD2 and AtCSLD3 together (Figure 1a). The open reading frames of SoCSLD2 and SoCSLD3 had 3444 and 3459 nucleotides, respectively. They encoded two putative proteins containing 1447 and 1152 amino acid residues with similar molecular mass (128,557 Da and 130,011 Da) and pI (6.9 and 7.06), respectively. Pairwise comparison analysis showed that SoCSLD2 and SoCSLD3 exhibited 80% and 81% identity to both AtCSLD2 and AtCSLD3 (Figure 1b), respectively. In addition, the conserved domain analysis showed that SoCSLD2 and SoCSLD3 proteins had the conserved DDDQ/RxxRW motif [21], which indicated they belonged to the CSL family (Figure 1b).

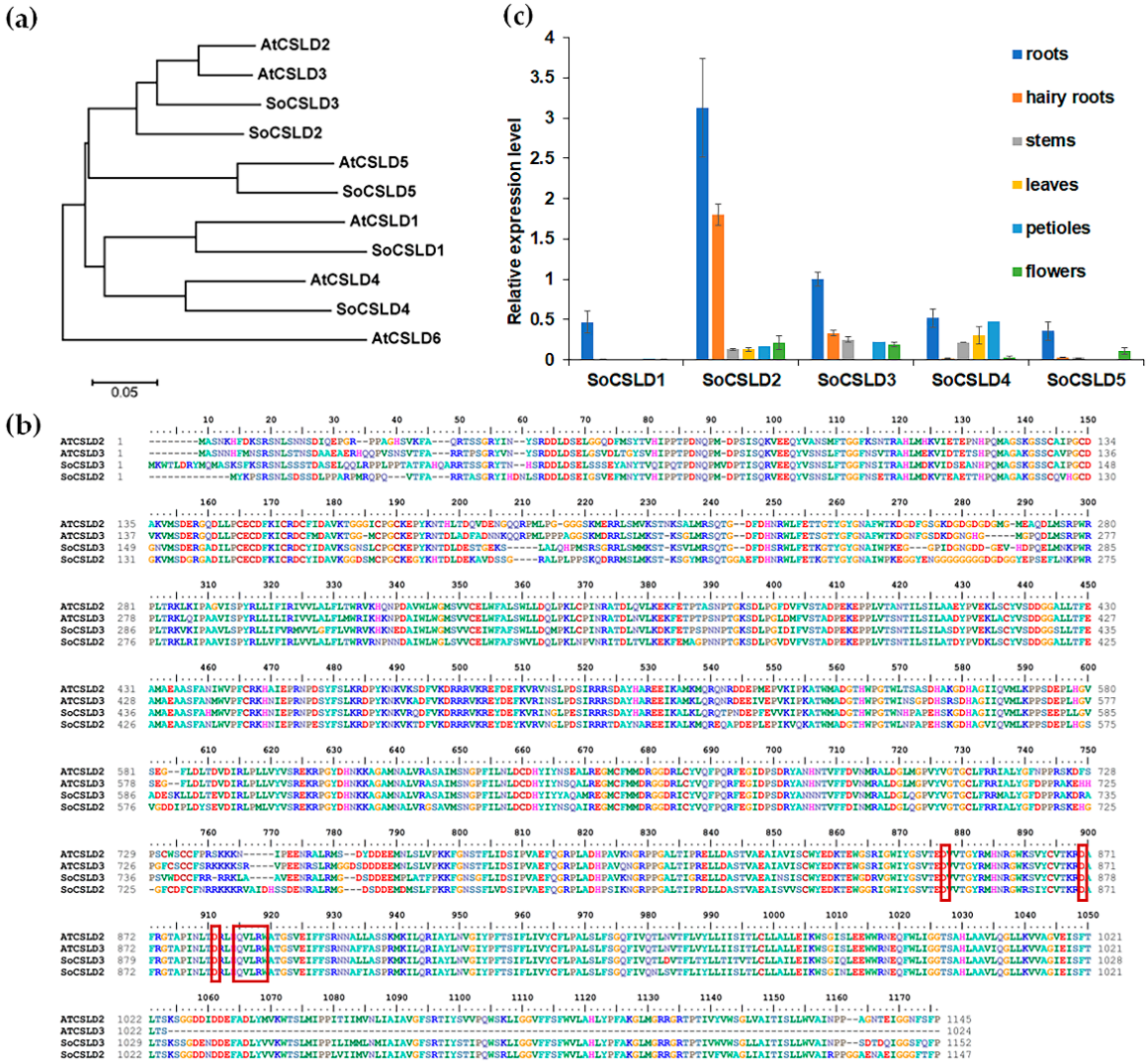

Figure 1. Bioinformatic analysis of SoCSLD2 and SoCSLD3 and expression analysis of the five predicted CSLD genes. (**a**) Joined phylogenetic tree of CSLD members in spinach and Arabidopsis was constructed with MEGA 4.0 by the neighbor-joining (NJ) method with 1000 bootstrap replicates. (**b**) Amino acid sequence alignment of SoCSLD2, SoCSLD3, AtCSLD2, and AtCSLD3. The identical and similar amino acid residues were present with same color, respectively. The conserved motif is labeled with red frame. (**c**) The qRT-PCR detection of the expression of five genes (*SoCSLD1*, *SoCSLD2*, *SoCSLD3*, *SoCSLD4*, and *SoCSLD5*) in the stem, leaf, flower, stipe, root, and hairy root of spinach. The relative mRNA abundance of each gene in all samples was normalized with respect to reference gene *Spo23599*, an actin gene of spinach.

The expression level of five SoCSLD genes in stems, roots, leaves, petioles, and flowers from two-month-old seedlings of spinach, as well as in hairy roots, were examined using qRT-PCR analysis. *SoCSLD2* and *SoCSLD3* were expressed in all these organs with similar patterns, and both of them showed obviously higher expressions in roots and hairy roots, respectively (Figure 1c). Especially, the expression of *SoCSLD2* was significantly higher in roots and root hairs than that in other organs and tissues (Figure 1c). In addition, the other genes (*SoCSLD1*, *SoCSLD4*, and *SoCSLD5*) were expressed in roots at relatively lower levels when compared with *SoCSLD2* and *SoCSLD3*.

The phylogenetic relationship and expression pattern of *SoCSLD2* and *SoCSLD3* indicates that they are good candidate genes for function analysis in hairy roots using CRISPR/Cas9 gene-editing system.

3.2. CRISPR/Cas9 Vector Construction and Co-Transformation Efficiency in Hairy Roots

Partial sequences of *SoCSLD2* and *SoCSLD3* were amplified from cDNA of roots. Three targets were designed for each gene. The tRNA–gRNA cassette strategies were used to construct the CRISPR/Cas9 vector (Supplementary Figure S1) [30].

T-DNA of binary vector harboring *Cas9*, tRNA–gRNA, and *bar* expression cassette were transferred into leaf explants of spinach using *A. rhizogenes* strain LBA9402. Hairy roots appeared after 10–20 days of infection (Figure 2a). Numerous independent hairy root lines were produced for each construct (22 root lines for *SoCSLD3* and 16 for *SoCSLD2*). The hairy root lines that could amplify the three genes (i.e., *Bar*, *Cas9*, and *rol B*) were considered to be the co-transformed lines. PCR detection indicated that *rolB*, *Cas9*, and *bar* genes were successfully transformed into spinach; 15 lines were obtained from 22 hairy root lines of *SoCSLD3*, and 15 lines were identified among 16 hairy root lines of *SoCSLD2* (Figure 2b,c).

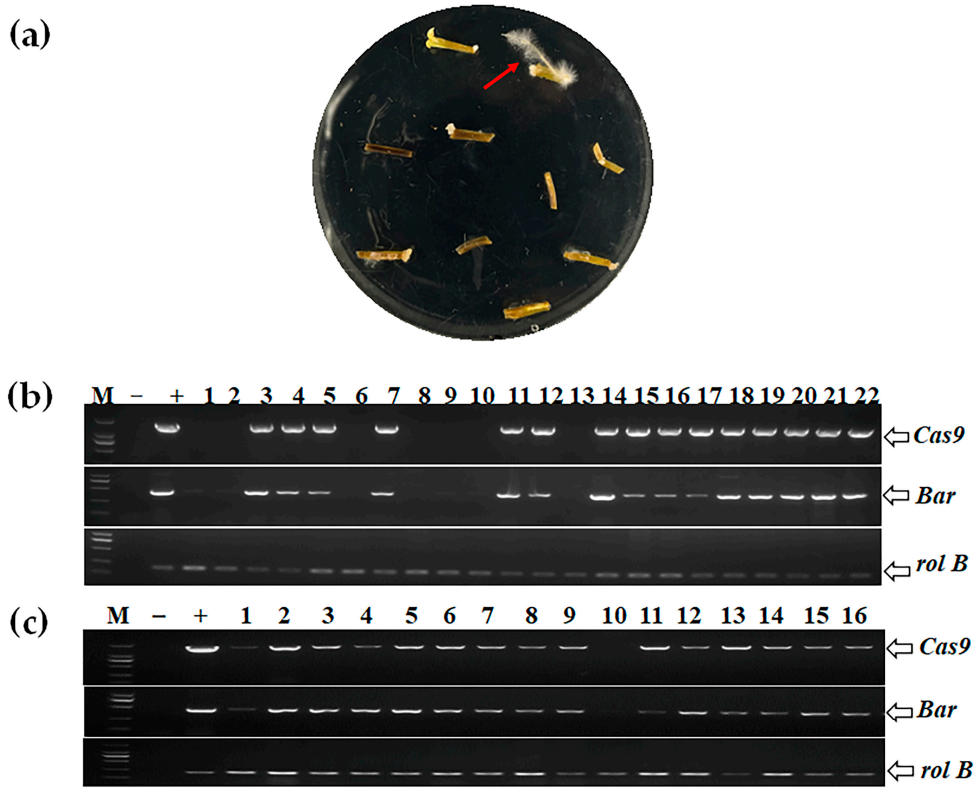

Figure 2. PCR analysis for identification of T-DNA transformed spinach hair roots. (**a**) Hairy roots appeared after 10–20 days of infection. (**b**,**c**) Identification of transgene hairy root lines of *SoCSLD3* (**b**) and *SoCSLD3* (**c**) by genome PCR screening. Untransformed roots served as a negative control, and *A. rhizogenes* strain LBA9402 harboring the CRISPR/Cas9 plasmid was used as a positive control. The expected band sizes of the *Bar*, *Cas9*, and *rol B* were marked by arrows.

3.3. Genotyping and Phenotyping of Edited Hairy Root Lines of SoCSLD2

The sequencing results showed that 15 hairy root lines of *SoCSLD2* were edited by CRISPR/Cas9 system (Figure 3 and Supplementary Table S1), of which seven lines (i.e., line 2, line 3, line 4, line 8, line 12, line 13, and line 14) showed obvious phenotypes of short root hairs (Figure 3a,b). The root hairs on the middle and/or top of hairy roots from these lines were abnormal and looked like bulging balls (Figure 3a,b). Sequence analysis showed that all of seven lines were bi-allelic/homozygous mutant lines with edited sequence in the same or different target sites of two sister chromatids (Figure 3e and Supplementary Table S1). The root-hair density of seven lines was not changed when compared with that in normal hairy roots (Figure 3f). However, the lengths of root hairs in seven lines were significantly reduced, to one-twentieth of the normal length (Figure 3g). The left eight transgenic lines were heterozygous or chimeric mutated lines. Among them, five heterozygous mutant lines (i.e., line 5, line 6, line 7, line 9, and line 11) contained one mutation type in each line, two chimeric mutant lines (line 1 and line 10) had three or two mutation types in each line, and line 15 had a wide-type genotype in three target sites (Supplementary Table S1). All the heterozygous or chimeric mutant lines showed no difference in the length and density of root hairs when compared with normal hairy roots (Figure 3c–g).

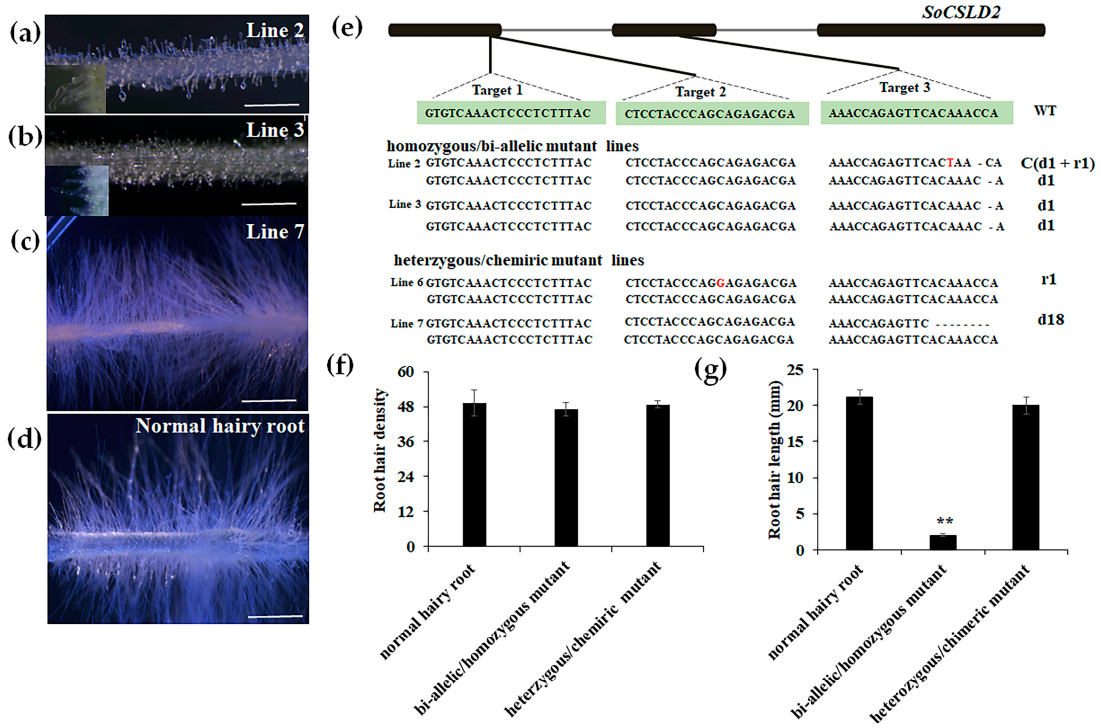

Figure 3. Phenotyping and genotyping of edited hairy root lines of *SoCSLD2*. (**a**,**b**) The phenotypes of bi-allelic line 2 (**a**) and homozygous line 3 (**b**) of *SoCSLD2*. Bar = 4 μm. (**c**) The phenotype of the heterozygous mutant line 7 of *SoCSLD2*. Bar = 20 μm. (**d**) The phenotype of the normal hairy root. Bar = 20 μm. (**e**) The mutation types of line 2, line 3, line 6, and line 7. The mutation types of each target were labeled in right of the target sites, respectively. Deletion bases were indicated by dashed lines; d#, number of bases deleted from the target site. Replacement bases were showed in red; r#, number of bases replaced at the target site; c, combined mutations (more than one mutation type in one allele). (**f**) Root-hair density and (**g**) root-hair length analysis of normal hairy roots, bi-allelic/homozygous mutant and heterozygous/chimeric mutant lines of hairy roots. Root-hair length and density were measured at the region 1.5 to 2 mm from the root tip. Root-hair density is shown as root hair number per mm^2; 24 roots of three lines (8 roots for each line) were measured for each mutation type, and the values were mean ± SD. Asterisk (**) indicates that difference is significant at $p < 0.01$.

3.4. Genotyping and Phenotyping of Edited Hairy Root Lines of SoCSLD3

Twenty-two hairy root lines were obtained for the gene *SoCSLD3*, among which fifteen lines were transgenic hairy root lines (Figure 2b). No lines showed obviously stunted root hairs. The 15 lines were submitted to target sequence analysis. No bi-allelic and homozygous mutants were obtained. All of them were either chimeric or heterozygous lines (Figure 4a–d and Supplementary Table S1). Among these lines, 13 lines (line 1 to line 13) were edited in more than one target sites; the remaining two lines (lines 14 and 15) had no changes at the target sites (Supplementary Table S1). The density and length of root hairs were similar with those of normal hairy roots (Figure 4e,f).

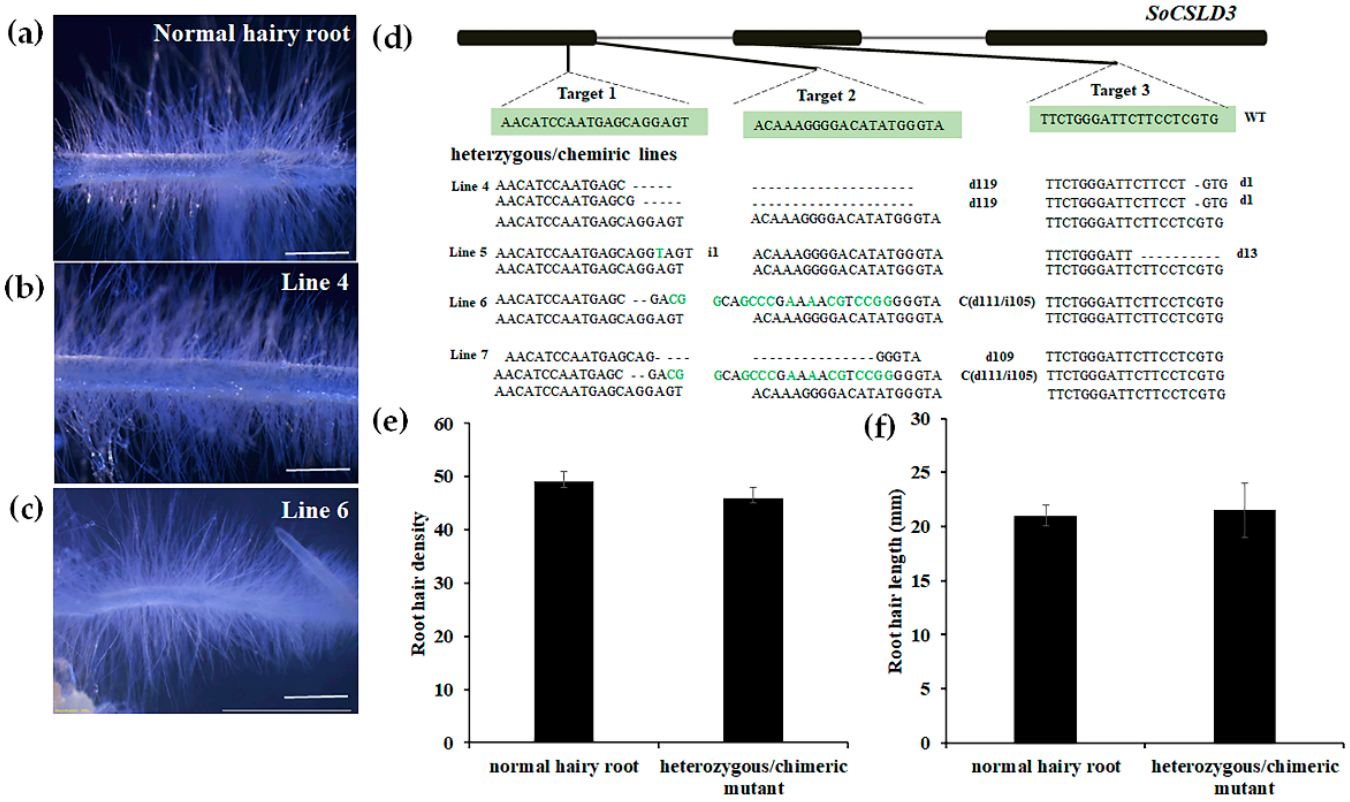

Figure 4. Phenotyping and genotyping of edited hairy root lines of *SoCSLD3*. (**a**–**c**) The root-hair phenotype of normal hairy root (**a**), line 4 (chimeric line) (**b**) and line 6 (heterozygous line) (**c**) of *SoCSLD3*. Bar = 20 μm. (**d**) The mutation types of the line 4, line 5, line 6, and line 7 (heterozygous mutated line). The mutation types of each target were labeled in right of the target sites, respectively. Deletion bases were indicated by dashed lines; d#, number of bases deleted from the target site. Insertion bases were marked in green; i#, number of bases inserted at the target site; c, combined mutations (more than one mutation type in one allele). (**e**) Root-hair density and (**f**) root-hair length analysis of normal hairy roots and heterozygous/chimeric mutant lines of hairy root. Root-hair length and density were measured at the region 1.5 to 2 mm from the root tip. Root-hair density is shown as root-hair number per mm^2; 24 roots of three lines (8 roots for each line) were measured for each mutation type, and the values were mean ± SD.

3.5. Mutation Variety and Frequency of CRISPR/Cas9-Edited Hairy Roots

To compare the CRISPR/Cas9 edit effectivity and mutation types at the target sites, 15 hairy root lines of *SoCSLD2* and *SoCSLD3* were subjected to PCR analyses, respectively. The PCR amplicons covering the target sites were sequenced (Table 1, Supplementary Sequencing Data). The PCR amplicons were further confirmed by TA cloning and sequencing (Supplementary Table S1, Supplementary Sequencing Data). The editing efficiency varies widely among the three targets of *SoCSLD2* and *SoCSLD3* (Table 1). For *SoCSLD2*, the third target site showed the highest mutation rate, which was 86.7% (13/15). Four mutation types were observed, in-

cluding replacement, insertion, deletion, and combined mutations (more than one mutation types in one target site). One line with the insertion, twelve lines with deletion, and two lines with combined mutations occurred at the third target site. Two lines with replacement and one line with deletion mutation occurred at the first target site. Only one line with replacement mutation occurred at the second target site (Table 1, Supplementary Table S1). For *SoCSLD3*, the first target site showed the highest mutation rate of 86.7% (13/15). Four mutation types appeared at the first target site, containing six insertion lines, two replacement lines, five deletions, and seven combined mutation lines. Two mutation types appeared at the second (four deletion and five combined mutation lines) and third target site (five deletion and five combined mutation lines) (Table 1, Supplementary Table S1).

Table 1. Detailed information of the mutation types of different targets in SoCSLD2 and SoCSLD3.

Gene	Number of Hairy Root Lines	Target Site/Sequence	GC Content (%)	Number of Hairy Root Lines with Mutation	Mutation Rate (%)	Number of Hairy Root Lines with Each Mutation Type			
						i	r	d	c
SoCSLD2	15	GTGTCAAACTCCCTCTTTAC	45	3	20.0	0	2	1	0
		CTCCTACCCAGCAGAGACGA	60	1	6.7	0	1	0	0
		AAACCAGAGTTCACAAACCA	40	13	86.7	1	0	12	2
SoCSLD3	15	AACATCCAATGAGCAGGAGT	45	13	86.7	6	2	5	7
		ACAAAGGGGACATATGGGTA	45	9	60.0	0	0	4	5
		TTCTGGGATTCTTCCTCGTG	50	8	53.3	0	0	5	5

i: insertion, d: deletion, r: replacement, c: combined mutation (more than one mutation type in one allele).

To detect the off-target events in CRISPR/Cas9 edited hairy roots of spinach, potential off-target loci following protospacer adjacent motif (PAM) sequences were predicted using the program written by Li et al. [31]. They were highly homologous with no more than three mismatches of each target sequence in the hairy roots of *SoCSLD2* and *SoCSLD3* (Supplementary Table S2; Supplementary Sequencing Data). Only one off-target locus was predicted in the first and second target sequence of *SoCSLD2*, respectively. However, five off-target loci were found in the third target sequence of *SoCSLD2* (Supplementary Table S2; Supplementary Sequencing Data). For *SoCSLD3*, there were one and two off-target sequences in the first and second target sequence, respectively. To examine whether these predictions were supported by our results, 15 hairy root lines of *SoCSLD2* and *SoCSLD3* were submitted for sequencing, respectively, and no site mutation was detected (Supplementary Table S2).

3.6. Transcriptomic Analysis of CRISPR/Cas9 Edited Hairy Roots

CSLD is critical to plant cell-wall development and dynamics, but its function in root-hair formation of spinach is still unclear. To clarify the function of *SoCSLD2* in regulating cell-wall dynamics in spinach root hairs, the transcriptomics analyses of *socsld2* mutant line 3 and normal hairy roots of spinach variety Sp75 were performed by using RNA-seq based on Illumina platform. A total of 25,495 unique genes were identified and quantified, 305 of which were more than 2.0-fold change ($p < 0.05$) in abundance and considered as the differentially expressed genes (DEGs) in hairy roots of *socsld2* mutant when compared with normal hairy roots. The hierarchical clustering indicated that 305 DEGs were clustered into two main groups (Cluster I and II) (Figure 5a and Supplementary Table S3). Metascape analysis showed that 13 GO biological processes of the corresponding genes were enriched (Figure 5b,c and Supplementary Table S4). Cluster I showed a significantly reduced pattern of 169 DEGs in *socsld2* mutants. The 57 reduced DEGs in Cluster I were enriched in 13 GO biological processes including biosynthesis of salicylic acid, phenylpropanoid, and flavonoid, response to salicylic acid, iron ion, bacterium, and hypoxia, metal ion and intercellular transports, defense response, and protein folding, as well as cell death (Figure 5b,c and Supplementary Table S4). Further, 136 DEGs in Cluster II were induced in *socsld2* mutants. Among them, 32 genes were enriched in response to various stresses (e.g., salicylic acid, iron ion, hypoxia, and bacterium), ion transport, cell death, as well as biosynthesis of flavonoid and phenylpropanoid (Figure 5b,c and Supplementary Table S4).

Interestingly, DEGs were highly enriched in several clusters, including the metal ion transport (blue node), salicylic acid biosynthesis (yellow node), hypoxia (green node), flavonoid biosynthesis (purple node), and host interaction and intercellular transport (orange and dark green nodes) (Figure 5b and Supplementary Table S4). In addition, these DEGs were enriched in several cellular components including cell wall, cell periphery, extracellular region, plasmodesma, plasma membrane, vacuole, and whole membrane (Figure 5d and Supplementary Table S5).

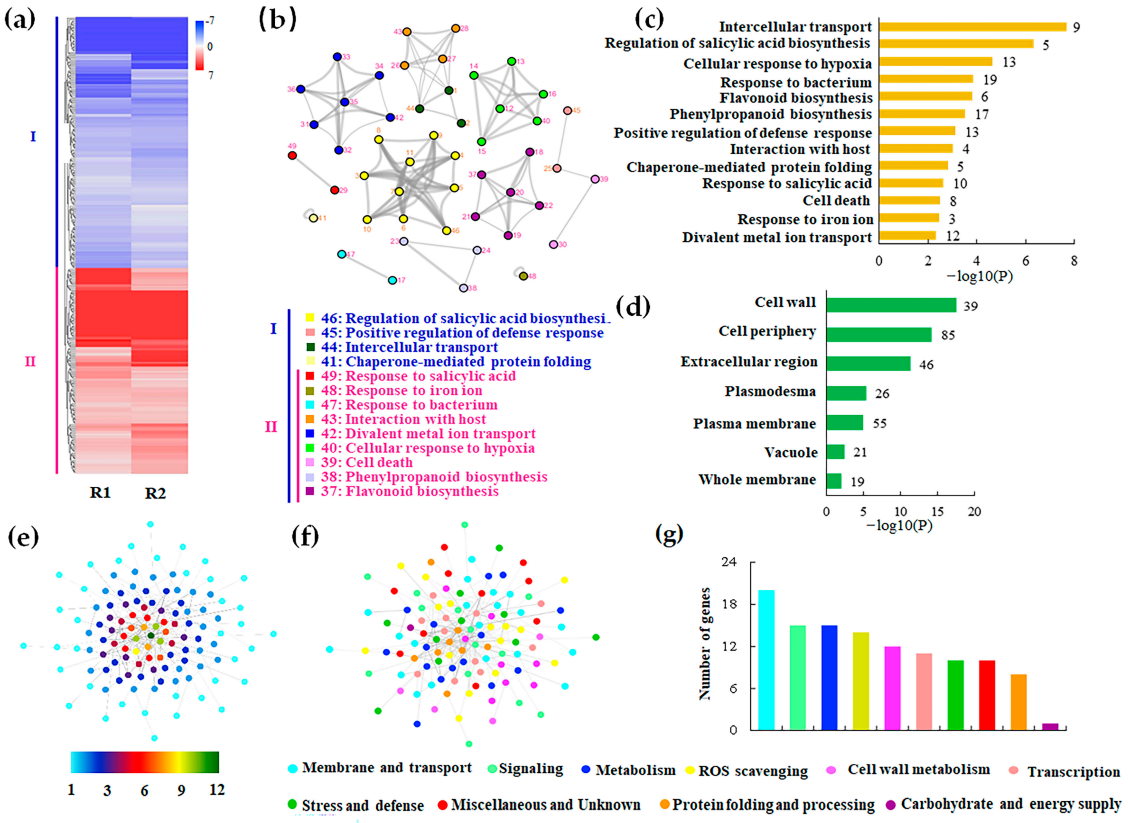

Figure 5. Cluster analysis and enrichment of differential expression genes (DEGs) and the predicted interaction networks of their encoding proteins in socsld2 mutants. (a) Hierarchical clustering analysis of DEGs. Two columns represent two replications of fold change of DEGs in socsld2 mutant (R1, R2). The rows represent individual genes. The increased or decreased genes are indicated in red or blue, respectively. The detailed information is listed in Supplemental Table S3. (b) Network of enriched terms of GO biological processes and KEGG pathways across the DEG lists of the two clusters. Each node represents an enriched term. The term genes next to the nodes are shown in Supplemental Table S4. The terms with a similarity > 0.3 are connected by edges. The same color nodes represent a subset of enriched terms, where the terms with the best p-values are highlighted with bold words. The color of the term genes (i.e., blue and pink) correspond to Cluster I and Cluster II, respectively. (c) Bar graph showing the summary of subsets enriched according to GO biological processes and KEGG pathways. The number in right represents number of DEGs enriched in each subset. (d) Enrichment analysis for cellular components of DEGs by GO annotation. The number on right represents number of DEGs enriched in each term. (e,f) Predicted interaction networks of proteins encoding by DEGs. Proteins (nodes) are shown as bubbles filled with different colors. The related interactions (edges) between proteins are shown as gray lines. (e) Heatmaps representing the node degree of each protein in the interaction network, respectively. The range of degree distribution is shown as a color gradient from light blue to dark green. (f) Proteins encoding by DEGs in various function categories, which are indicated by the node fill color. (g) Numbers of proteins encoding by DEGs in different function categories.

To predict the relationship of DEGs in *socsld2* mutant roots, the Arabidopsis homologs of spinach proteins encoding by DEGs were found by sequence BLASTing in TAIR database (Supplementary Table S6) and then were subjected to the web-tool SRING 10 for predicting protein–protein interaction (PPI) networks. The network showed 116 nodes (representing proteins encoded by DEGs) with 172 node degrees (representing PPIs) in *socsld2* mutants (Figure 5e and Supplementary Table S7). In this network, the dark-green nodes represent cinnamyl alcohol dehydrogenase 3, calmodulin-binding protein 60-C, receptor-like protein kinase, and 70 kDa heat shock protein, with more than 10 node degrees for each, implying their complicated interaction with other proteins. Interestingly, the nodes representing proteins for cell-wall metabolism, protein folding and processing, membrane and transport, and signaling have more node degrees than other nodes, suggesting that these signal and metabolic processes were affected in mutants (Figure 5f,g, and Supplementary Table S7).

4. Discussion

4.1. The tRNA–gRNA Cassette Expression System Is an Efficient Tool for Multiplex Targeted Mutagenesis in Spinach

In the past years, diverse CRISPR/Cas-based gene editing systems have been widely used to modify plant genomes, which facilitate the molecular genetics analysis and breeding [32,33]. However, it is not reported in spinach. In this study, on the basis of *A. rhizogenes*-mediated hairy root platform established by us previously [3], we selectively modified the genome of spinach hairy roots using the plant codon-optimized *Streptococcus pyogenes* CRISPR-associated protein 9 (SpCas9) and *AtU3b* promoter. Our results revealed that 27 of 30 hairy root lines were edited successfully, which indicated that the SpCas9 and *AtU3b* promoter worked efficiently in spinach (Table 1). All the six target sites of *SoCSLD2* and *SoCSLD3* were edited to diverse mutation types, including substitution, insertion, combined mutation, and deletion, and the highest mutation frequency reached to 86.7% (Table 1). The high editing efficiency resulted from the tRNA–gRNA cassette expression system and multiple target sequences for each gene, since tRNA not only serves as an enhancer for AtU3b, but also as a "divider" for the sgRNAs [34,35].

The mutation frequencies of different targets were varied in our results and were likely affected by many factors. It was reported that GC percentage of overall targets [36] and the 6-PAM-proximal nucleotides [37] were positively associated with editing efficiency in zebrafish (*Danio rerio*) and Drosophila, respectively. In this preliminary study, the GC contents of the six target sites ranged from 40% to 60%, which has been reported to be favored for efficient on-target cleavage [38]. For *SoCSLD2*, the GC content of the first, second, and third target sequence was 45%, 60%, and 40%, while the GC contents of the first, second, and third target sequence of *SoCSLD3* were 45%, 45%, and 50%, respectively. However, the highest mutation rate occurred in the third target site of *SoCSLD2* and the first target sequence of *SoCSLD3*, which have the lowest GC content both in the target sequences (40% and 45%) and in the 6-PAM-proximal nucleotides (2/6 and 3/6). However, this is not consistent with the previous notion [36–38], which needs to be further investigated.

In fact, the modulation of mutation efficiency of the CRISPR/Cas9 system was sophisticated and fine-tuned by diverse factors, such as the promoter used to drive sgRNA expression [39], the efficiency of gRNA to search and target to the specific site [40], the T-DNA insertion site in genome [41], as well as the transformation method [42]. In addition, the mutation ratio of CRISPR/Cas system was variable in different plant species [43–46]. Importantly, the secondary structure and purine residues in the gRNA end can influence gRNA effectiveness and then affect gene-editing efficiency. A pool of sgRNAs and online tools have been reported that have facilitated sgRNA design for gene editing [47]. In the future, we will optimize the promoter (e.g., U3/U6 promoter from spinach) [39], the design of highly active sgRNAs for certain genes [47], the distance between two gRNAs [35], and the protoplast expression system [42] to improve the CRIPSR/Cas9 editing efficiency in spinach.

4.2. SoCSLD2 Regulates the Spinach Root-Hair Growth

CSLD family members encode glycosyltransferases that are responsible for the synthesis of the glycan backbones of cellulose and most polysaccharides, which have been proven to be pivotal for plant cell-wall development [21]. Arabidopsis *AtCSLD* family has six members, which regulate the growth of stems, roots, and pollen tubes [17,48]. Among them, *AtCSLD2* and *AtCSLD3* are required for proper root-hair growth [25,49,50]. However, the function of *SoCSLDs* in spinach hairy roots is still unknown.

In this study, five *SoCSLDs* were found in spinach genome. The analyses of phylogenetic tree and homology alignment indicated that *SoCSLD2* and *SoCSLD3* were the homologs of *AtCSLD3* and *AtCSLD2* (Figure 1a). We found that *SoCSLD2* and *SoCSLD3* were highly expressed in roots and hairy roots of spinach (Figure 1c), which was similar to the highest expression of *AtCSLD3* and *AtCSLD2* in Arabidopsis roots [22,24]. Two poplar genes (*PdCSLD5* and *PdCSLD6*) also had high similarity to *AtCSLD2* and *AtCSLD3* [23]. Overexpression of *PdCSLD5* and *PdCSLD6* can rescue the root-hair defect phenotype of *atcsld3* mutant [23]. Recently, several homozygous of *AtCSLD2* and *AtCSLD3* (e.g., *GhCSLD3*, *PtrCSLD5*, and *LjCSLD1*) have been reported as conserved with *AtCSLD2* and *AtCSLD3* in regulating the root-hair development [26–29].

In our study, all the bi-allelic or homozygous mutants of *SoCSLD2* being generated by CRISPR/Cas9 system exhibited short and/or bulking root hairs. However, the root-hair numbers were not changed compared with the wild-type (Figure 3). Importantly, the phenotype of these lines was stable during the four-month subculturing process. This indicates that *SoCSLD2* has more similar function to *AtCSLD2* than *AtCSLD3*. However, in our study, all these CRISPR/Cas9-edited lines of *SoCSLD3* were either chimeric or heterozygous, such that no stable root-hair phenotype was observed (Figure 4). Even so, we attempted to repeat this experiment to obtain bi-allelic or homozygous mutated lines for *SoCSLD3*. Unfortunately, there were still no lines showing a similar phenotype with *atcsld3* mutant, although 17 transgenic lines were induced (data not shown). Therefore, we suspect that the homozygous or bi-allelic mutation of *SoCSLD3* would result in growth inhibition of hairy roots, which is similar to the phenotype of root hair loss in *atcsld3* mutants [24]. However, the homolog relationship of *SoCSLD3* and *AtCSLD3* still needs to be further investigated by observing root-hair phenotypes and detecting cell-wall cellulose composition in plant mutation and complementary materials.

4.3. SoCSLD2 Is Involved in Cell-Wall Remodulation in Hairy Roots of Spinach

CSLDs are essential for the synthesis of polymers, which is critical for the fast-growing primary cell wall at the tip of root hairs [21,22,25]. For example, the root-hair-tip-localized AtCSLD3 was predicted to regulate root-hair elongation and cell integrity [24]. In the *atcsld3* mutant, the cell wall changed at the site of root hair tip, leading to the inhibition of root-hair elongation [24].

In this study, to evaluate the function of spinach *SoCSLD2* (a candidate homolog of *AtCSLD2*), we obtained the homozygous *socsld2* mutant using the CRISPR/Cas9-based gene editing system. The transcriptomics analysis was performed using hairy roots from *socsld2* mutants and the normal hairy roots of spinach variety Sp75. The transcriptomic results indicated that the expression patterns of 305 genes were significantly disturbed in *socsld2* mutants, which might affect the root-hair phenotype (Figure 5).

In the *socsld2* mutant, the expression levels of some expansins and xyloglucan endotransglucosylase/hydrolases (XTH) were increased, which could enhance the dissociation of polysaccharide complex and adjustment of xyloglucans, respectively [51], therefore resulting in cell-wall relaxation and extension. Moreover, the increase of plasma membrane H^+-ATPase could facilitate extracellular acidification-activating expansin activity [51]. The increased endo-β-1,3-glucanase and β-1,3-1,4-glucanase may induce the hydrolysis of the glucan polymer cross-links [52,53], and the decrease of arabinogalactan proteins showed potential for reducing the cross-link of pectin and arabinoxylan impairing wall-thickening [54,55]. All these changes implied that cell-wall loosening was enhanced, while

its strength was reduced in mutants. On the other hand, the decrease of galacturonosyltransferase (GAUT) could affect pectin synthesis, and the increase of pectin acetylesterase had capacity to induce the cleavage of the acetylester bond from pectin [56,57], which might inhibit pectin synthesis and reduce cell-wall rigidity in the *socsld2* mutant. Importantly, the changes of three lignin synthesis-related genes, encoding cinnamyl alcohol dehydrogenase, hydroxycinnamoyl CoA quinate hydroxycinnamoyl transferase, and laccase, suggested that the disturbance of lignin in cell wall could affect the root-hair growth [58,59]. Additionally, the enrichment of a number of genes was involved in various stress responses (e.g., ion ions, hypoxia, and bacterium), signaling, transcription, protein folding and processing, ROS scavenging, and energy metabolism. This suggests that the knockout of *SoCSLD2* could result in cell-wall change and series modulations in signal transduction, gene expression regulation, and various metabolisms, which may lead to inhibition of root hair growth in *socsld2* mutant.

5. Conclusions

Currently, the spinach genome is published [1,2]. A large number of genes/proteins have been proposed to be critical for spinach development and stress tolerance using genome-wide gene identification and proteomics analyses [5–7,60]. It is important to breed more novel spinach varieties with excellent agronomic traits, such as low oxalic acid content, high temperature tolerance, downy mildew resistant, and suitability for mechanical harvesting. Thus, the genetic transformation system is necessary for spinach studies.

In this study, our preliminary results indicated that the CRISPR/Cas9 via tRNA–sgRNA strategy was an efficient tool for genome editing in spinach. Homozygous and bi-allelic mutations were induced by CRISPR/Cas9 in hairy roots of spinach, which provided a powerful tool to study gene function in spinach roots. In the future, we will develop an efficient callus-based regeneration system for molecular genetics analysis. Also, we will develop diverse CRISPR/Cas systems to enhance their editing accuracy and efficiency for facilitating their application in spinach molecular design breeding.

Supplementary Materials: The following supporting information can be downloaded at: https://www.mdpi.com/article/10.3390/horticulturae8080735/s1, Figure S1: Schematic illustration of CRISPR/Cas9 vector for *SoCSLD2* and *SoCSLD3*. Figure S2: The Sanger sequencing data of PCR products with mixed peaks and/or sequence changes in the target sites. Figure S3: The protein sequence alignment analysis of WT, line 2 mutant, and line 3 of *SoCSLD2*. Table S1: Sequencing results of PCR amplicons from transgenic hairy roots lines of *SoCSLD2* and *SoCSLD3*. Table S2: The prediction of putative off-target loci and the detection of mutations at putative off-target sites. Table S3: List of annotation information of differentially expressed genes between normal wild-type (WT) and *socsld2* mutant (line 3). Table S4: Detailed information on pathway and process enrichment analysis carried out by GO biological processes and KEGG pathway. Table S5: Cellular component enrichment analysis for differentially expressed genes by GO annotation. Table S6: Homologs of differentially expressed genes in Arabidopsis found by sequence BLASTing in TAIR database. Table S7: Degree analysis of protein interaction network among proteins encoded by differentially expressed genes in *socsld2* mutant vs. normal wild type generated by STRING 10. Table S8: The primers used in this study. Sequencing Data: Sequencing data of *SoCSLD2* and *SoCSLD3* from *E. coli*.

Author Contributions: S.D. and C.F. planned and designed the research; Y.C., Y.X., Y.Z., H.Z. (Heng Zhang), Z.Q., C.B., H.Z. (Hailing Zhang), D.M. and Q.W. performed the research, analyzed, and interpreted data; and Y.C., C.F., M.S. and S.D. wrote the manuscript. All authors have read and agreed to the published version of the manuscript.

Funding: This study was supported by the Foundation of Shanghai Science and Technology Committee, China (No. 17391900600) and the Fund of Shanghai Engineering Research Center of Plant Germplasm Resources (No. 17DZ2252700) to S.D., the National Nature Science Foundation of China (No. 31902012) to M.S., and QIBEBT and Dalian National Laboratory for Clean Energy (DNL), CAS (No. QIBEBT I201921) to C.F.

Institutional Review Board Statement: Not applicable.

Informed Consent Statement: Not applicable.

Data Availability Statement: Not applicable.

Acknowledgments: We are grateful to Yao-Guang Liu (Huanan Agricultural University, China) for kindly providing the whole set of CRISPR/Cas9 vectors including pYLCRISPR/Cas9 35s-B and pYLsgRNA-AtU3b. We also thank Ying Lu (Shanghai Ocean University, China) for helping off-target search, including program modification and debugger, looking for off-target positions on chromosomes in spinach by BLAST tool, and off-target sequence extraction.

Conflicts of Interest: No conflict of interest exits in the submission of this manuscript, and manuscript is approved by all authors for publication. The work described was original research that has not been published previously, and not under consideration for publication elsewhere, in whole or in part. All the authors listed have approved the manuscript that is enclosed.

References

1. Xu, C.; Jiao, C.; Sun, H.; Cai, X.; Wang, X.; Ge, C.; Zheng, Y.; Liu, W.; Sun, X.; Xu, Y.; et al. Draft genome of spinach and transcriptome diversity of 120 Spinacia accessions. *Nat. Commun.* **2017**, *8*, 15275. [CrossRef] [PubMed]
2. Cai, X.; Sun, X.; Xu, C.; Sun, H.; Wang, X.; Ge, C.; Zhang, Z.; Wang, Q.; Fei, Z.; Jiao, C.; et al. Genomic analyses provide insights into spinach domestication and the genetic basis of agronomic traits. *Nat. Commun.* **2021**, *12*, 7246. [CrossRef] [PubMed]
3. Xu, Y.; Cao, Y.P.; Wang, Y.; Fu, C.; Dai, S. *Agrobacterium rhizogenes*-mediated transformation system of Spinacia oleracea. *Chin. Bull. Bot.* **2019**, *54*, 515–521. [CrossRef]
4. Ge, C.; Cai, X.; Xu, C.; Wang, X.; Deng, J.; Liu, S.; Zhao, Q.; Dai, S.; Wang, Q. A new heat-resistant spinach cultivar 'Hubo 1'. *Acta Hortic. Sin.* **2015**, *42*, 399–400. [CrossRef]
5. Zhao, Q.; Chen, W.; Bian, J.; Xie, H.; Li, Y.; Xu, C.; Ma, J.; Guo, S.; Chen, J.; Cai, X.; et al. Proteomics and Phosphoproteomics of Heat Stress-Responsive Mechanisms in Spinach. *Front. Plant Sci.* **2018**, *9*, 800. [CrossRef]
6. Li, S.; Yu, J.; Li, Y.; Zhang, H.; Bao, X.; Bian, J.; Xu, C.; Wang, X.; Cai, X.; Wang, Q.; et al. Heat-Responsive Proteomics of a Heat-Sensitive Spinach Variety. *Int. J. Mol. Sci.* **2019**, *20*, 3872. [CrossRef]
7. Li, Y.; Zhang, H.; Zhang, Y.; Liu, Y.; Li, Y.; Tian, H.; Guo, S.; Sun, M.; Qin, Z.; Dai, S. Genome-wide identification and expression analysis reveals spinach brassinosteroid-signaling kinase (BSK) gene family functions in temperature stress response. *BMC Genom.* **2022**, *23*, 453. [CrossRef]
8. Barrangou, R.; Marraffini, L.A. CRISPR-Cas Systems: Prokaryotes Upgrade to Adaptive Immunity. *Mol. Cell* **2014**, *54*, 234–244. [CrossRef]
9. Jinek, M.; Chylinski, K.; Fonfara, I.; Hauer, M.; Doudna, J.A.; Charpentier, E. A Programmable dual-RNA-guided DNA endonuclease in adaptive bacterial immunity. *Science* **2012**, *337*, 816–821. [CrossRef]
10. Ma, X.; Liu, Y. CRISPR/Cas9-Based Multiplex Genome Editing in Monocot and Dicot Plants. *Curr. Protoc. Mol. Biol.* **2016**, *115*, 31.6.1–31.6.21. [CrossRef]
11. Dong, F.; Xie, K.; Chen, Y.; Yang, Y.; Mao, Y. Polycistronic tRNA and CRISPR guide-RNA enables highly efficient multiplexed genome engineering in human cells. *Biochem. Biophys. Res. Commun.* **2017**, *482*, 889–895. [CrossRef]
12. Wang, P.; Zhang, J.; Sun, L.; Ma, Y.; Xu, J.; Liang, S.; Deng, J.; Tan, J.; Zhang, Q.; Tu, L.; et al. High efficient multisites genome editing in allotetraploid cotton (*Gossypium hirsutum*) using CRISPR/Cas9 system. *Plant Biotechnol. J.* **2018**, *16*, 137–150. [CrossRef]
13. Gao, C. Genome engineering for crop improvement and future agriculture. *Cell* **2021**, *184*, 1621–1635. [CrossRef]
14. Zhu, H.; Li, C.; Gao, C. Applications of CRISPR–Cas in agriculture and plant biotechnology. *Nat. Rev. Mol. Cell Biol.* **2020**, *11*, 661–677. [CrossRef]
15. Georgiev, M.I.; Agostini, E.; Ludwig-Müller, J.; Xu, J. Genetically transformed roots: From plant disease to biotechnological resource. *Trends Biotechnol.* **2012**, *30*, 528–537. [CrossRef]
16. Libault, M.; Brechenmacher, L.; Cheng, J.; Xu, D.; Stacey, G. Root hair systems biology. *Trends Plant Sci.* **2010**, *15*, 641–650. [CrossRef]
17. Yin, L.; Verhertbruggen, Y.; Oikawa, A.; Manisseri, C.; Knierim, B.; Prak, L.; Jensen, J.K.; Knox, J.P.; Auer, M.; Willats, W.G.; et al. The Cooperative Activities of CSLD2, CSLD3, and CSLD5 Are Required for Normal *Arabidopsis* Development. *Mol. Plant* **2011**, *4*, 1024–1037. [CrossRef]
18. Lampugnani, E.R.; Khan, G.A.; Somssich, M.; Persson, S. Building a plant cell wall at a glance. *J. Cell Sci.* **2018**, *131*, jcs207373. [CrossRef]
19. Lampugnani, E.R.; Sandoval, E.F.; Tan, Q.W.; Mutwil, M.; Bowman, J.L.; Persson, S. Cellulose Synthesis—Central Components and Their Evolutionary Relationships. *Trends Plant Sci.* **2019**, *24*, 402–412. [CrossRef]
20. Lerouxel, O.; Cavalier, D.M.; Liepman, A.; Keegstra, K. Biosynthesis of plant cell wall polysaccharides—A complex process. *Curr. Opin. Plant Biol.* **2006**, *9*, 621–630. [CrossRef]
21. Richmond, T.A.; Somerville, C.R. The Cellulose Synthase Superfamily. *Plant Physiol.* **2000**, *124*, 495–498. [CrossRef] [PubMed]

22. Bernal, A.J.; Yoo, C.-M.; Mutwil, M.; Jensen, J.K.; Hou, G.; Blaukopf, C.; Sørensen, I.; Blancaflor, E.B.; Scheller, H.V.; Willats, W.G. Functional Analysis of the Cellulose Synthase-Like Genes *CSLD1*, *CSLD2*, and *CSLD4* in Tip-Growing *Arabidopsis* Cells. *Plant Physiol.* **2008**, *148*, 1238–1253. [CrossRef] [PubMed]
23. Qi, G.; Hu, R.; Yu, L.; Chai, G.; Cao, Y.; Zuo, R.; Kong, Y.; Zhou, G. Two poplar cellulose synthase-like D genes, PdCSLD5 and PdCSLD6, are functionally conserved with *Arabidopsis* CSLD3. *J. Plant Physiol.* **2013**, *170*, 1267–1276. [CrossRef] [PubMed]
24. Favery, B.; Ryan, E.; Foreman, J.; Linstead, P.; Boudonck, K.; Steer, M.; Shaw, P.; Dolan, L. *KOJAK* encodes a cellulose synthase-like protein required for root hair cell morphogenesis in *Arabidopsis*. *Genes Dev.* **2001**, *15*, 79–89. [CrossRef] [PubMed]
25. Yoo, C.-M.; Quan, L.; Blancaflor, E.B. Divergence and Redundancy in CSLD2 and CSLD3 Function During *Arabidopsis* Thaliana Root Hair and Female Gametophyte Development. *Front. Plant Sci.* **2012**, *3*, 111. [CrossRef] [PubMed]
26. Hu, H.; Zhang, R.; Dong, S.; Li, Y.; Fan, C.; Wang, Y.; Xia, T.; Chen, P.; Wang, L.; Feng, S.; et al. AtCSLD3 and GhCSLD3 mediate root growth and cell elongation in downstream of ethylene response pathway in *Arabidopsis*. *J. Exp. Bot.* **2018**, *69*, 1065–1080. [CrossRef]
27. Hu, H.; Zhang, R.; Tang, Y.; Peng, C.; Wu, L.; Feng, S.; Chen, P.; Wang, Y.; Du, X.; Peng, L. Cotton CSLD3 restores cell elongation and cell wall integrity mainly by enhancing primary cellulose production in the *Arabidopsis* cesa6 mutant. *Plant Mol. Biol.* **2019**, *101*, 389–401. [CrossRef]
28. Peng, X.; Pang, H.; Abbas, M.; Yan, X.; Dai, X.; Li, Y.; Li, Q. Characterization of Cellulose synthase-like D (CSLD) family revealed the involvement of PtrCslD5 in root hair formation in *Populus trichocarpa*. *Sci. Rep.* **2019**, *9*, 1452. [CrossRef]
29. Karas, B.J.; Ross, L.; Novero, M.; Amyot, L.; Shrestha, A.; Inada, S.; Nakano, M.; Sakai, T.; Bonetta, D.; Sato, S.; et al. Intragenic complementation at the *Lotus japonicus* CELLULOSE SYNTHASE-LIKE D1 locus rescues root hair defects. *Plant Physiol.* **2021**, *186*, 2037–2050. [CrossRef]
30. Xie, K.; Minkenberg, B.; Yang, Y. Boosting CRISPR/Cas9 multiplex editing capability with the endogenous tRNA-processing system. *Proc. Natl. Acad. Sci. USA* **2015**, *112*, 3570–3575. [CrossRef]
31. Li, B.; Cui, G.; Shen, G.; Zhan, Z.; Huang, L.; Chen, J.; Qi, X. Targeted mutagenesis in the medicinal plant *Salvia miltiorrhiza*. *Sci. Rep.* **2017**, *7*, srep43320. [CrossRef]
32. Gupta, D.; Bhattacharjee, O.; Mandal, D.; Sen, M.K.; Dey, D.; Dasgupta, A.; Kazi, T.A.; Gupta, R.; Sinharoy, S.; Acharya, K.; et al. CRISPR-Cas9 system: A new-fangled dawn in gene editing. *Life Sci.* **2019**, *232*, 116636. [CrossRef]
33. Li, Y.; Li, S.; Wang, J.; Liu, G. CRISPR/Cas Systems towards Next-Generation Biosensing. *Trends Biotechnol.* **2019**, *37*, 730–743. [CrossRef]
34. Wang, Z.; Liu, X.; Xie, X.; Deng, L.; Zheng, H.; Pan, H.; Li, D.; Li, L.; Zhong, C. ABE8e with Polycistronic tRNA-gRNA Expression Cassette Sig-Nificantly Improves Adenine Base Editing Efficiency in *Nicotiana benthamiana*. *Int. J. Mol. Sci.* **2021**, *22*, 5663. [CrossRef]
35. Qi, W.; Zhu, T.; Tian, Z.; Li, C.; Zhang, W.; Song, R. High-efficiency CRISPR/Cas9 multiplex gene editing using the glycine tRNA-processing system-based strategy in maize. *BMC Biotechnol.* **2016**, *16*, 58. [CrossRef]
36. Gagnon, J.A.; Valen, E.; Thyme, S.B.; Huang, P.; Ahkmetova, L.; Pauli, A.; Montague, T.G.; Zimmerman, S.; Richter, C.; Schier, A.F. Efficient Mutagenesis by Cas9 Protein-Mediated Oligonucleotide Insertion and Large-Scale Assessment of Single-Guide RNAs. *PLoS ONE* **2014**, *9*, e98186. [CrossRef]
37. Ren, X.; Yang, Z.; Xu, J.; Sun, J.; Mao, D.; Hu, Y.; Yang, S.-J.; Qiao, H.-H.; Wang, X.; Hu, Q.; et al. Enhanced Specificity and Efficiency of the CRISPR/Cas9 System with Optimized sgRNA Parameters in *Drosophila*. *Cell Rep.* **2014**, *9*, 1151–1162. [CrossRef]
38. Liu, X.; Homma, A.; Sayadi, J.; Yang, S.; Ohashi, J.; Takumi, T. Sequence features associated with the cleavage efficiency of CRISPR/Cas9 system. *Sci. Rep.* **2016**, *6*, 19675. [CrossRef]
39. Zhou, Z.; Tan, H.; Li, Q.; Chen, J.; Gao, S.; Wang, Y.; Chen, W.; Zhang, L. CRISPR/Cas9-mediated efficient targeted mutagenesis of RAS in *Salvia miltiorrhiza*. *Phytochemistry* **2018**, *148*, 63–70. [CrossRef]
40. Johnson, R.A.; Gurevich, V.; Filler, S.; Samach, A.; Levy, A.A. Comparative assessments of CRISPR-Cas nucleases' cleavage efficiency in planta. *Plant Mol. Biol.* **2015**, *87*, 143–156. [CrossRef]
41. Shan, Q.; Wang, Y.; Li, J.; Zhang, Y.; Chen, K.; Liang, Z.; Zhang, K.; Liu, J.; Xi, J.J.; Qiu, J.-L.; et al. Targeted genome modification of crop plants using a CRISPR-Cas system. *Nat. Biotechnol.* **2013**, *31*, 686–688. [CrossRef] [PubMed]
42. Oh, Y.; Lee, B.; Kim, H.; Kim, S.-G. A multiplex guide RNA expression system and its efficacy for plant genome engineering. *Plant Methods* **2020**, *16*, 37. [CrossRef] [PubMed]
43. Feng, Z.; Zhang, B.; Ding, W.; Liu, X.; Yang, D.-L.; Wei, P.; Cao, F.; Zhu, S.; Zhang, F.; Mao, Y.; et al. Efficient genome editing in plants using a CRISPR/Cas system. *Cell Res.* **2013**, *23*, 1229–1232. [CrossRef] [PubMed]
44. Cai, Y.; Chen, L.; Liu, X.; Sun, S.; Wu, C.; Jiang, B.; Han, T.; Hou, W. CRISPR/Cas9-Mediated Genome Editing in Soybean Hairy Roots. *PLoS ONE* **2015**, *10*, e0136064. [CrossRef]
45. Fauser, F.; Schiml, S.; Puchta, H. Both CRISPR/Cas-based nucleases and nickases can be used efficiently for genome engineering in *Arabidopsis thaliana*. *Plant J.* **2014**, *79*, 348–359. [CrossRef]
46. Zhang, H.; Zhang, J.; Wei, P.; Zhang, B.; Gou, F.; Feng, Z.; Mao, Y.; Yang, L.; Zhang, H.; Xu, N.; et al. The CRISPR/Cas9 system produces specific and homozygous targeted gene editing in rice in one generation. *Plant Biotechnol. J.* **2014**, *12*, 797–807. [CrossRef]
47. Doench, J.G.; Hartenian, E.; Graham, D.B.; Tothova, Z.; Hegde, M.; Smith, I.; Sullender, M.; Ebert, B.L.; Xavier, R.J.; Root, D.E. Rational design of highly active sgRNAs for CRISPR-Cas9-mediated gene inactivation. *Nat. Biotechnol.* **2014**, *32*, 1262–1267. [CrossRef]

48. Wang, W.; Wang, L.; Chen, C.; Xiong, G.; Tan, X.-Y.; Yang, K.-Z.; Wang, Z.-C.; Zhou, Y.; Ye, D.; Chen, L.-Q. Arabidopsis CSLD1 and CSLD4 are required for cellulose deposition and normal growth of pollen tubes. *J. Exp. Bot.* **2011**, *62*, 5161–5177. [CrossRef]
49. Park, S.; Szumlanski, A.L.; Gu, F.; Guo, F.; Nielsen, E. A role for CSLD3 during cell-wall synthesis in apical plasma membranes of tip-growing root-hair cells. *Nat. Cell Biol.* **2011**, *13*, 973–980. [CrossRef]
50. Wang, X.; Cnops, G.; Vanderhaeghen, R.; De Block, S.; Van Montagu, M.; Van Lijsebettens, M. *AtCSLD3*, A Cellulose Synthase-Like Gene Important for Root Hair Growth in *Arabidopsis*. *Plant Physiol.* **2001**, *126*, 575–586. [CrossRef]
51. Cosgrove, D.J. Growth of the plant cell wall. *Nat. Rev. Mol. Cell Biol.* **2005**, *6*, 850–861. [CrossRef] [PubMed]
52. Thomas, B.R.; Inouhe, M.; Simmons, C.R.; Nevins, D.J. Endo-1,3;1,4-β-glucanase from coleoptiles of rice and maize: Role in the regulation of plant growth. *Int. J. Biol. Macromol.* **2000**, *27*, 145–149. [CrossRef]
53. Li, J.; Cao, C.; Jiang, Y.; Huang, Q.; Shen, Y.; Ni, J. A Novel Digestive GH16 β-1,3(4)-Glucanase from the Fungus-Growing Termite *Macrotermes barneyi*. *Appl. Biochem. Biotechnol.* **2020**, *192*, 1284–1297. [CrossRef] [PubMed]
54. Tan, L.; Eberhard, S.; Pattathil, S.; Warder, C.; Glushka, J.; Yuan, C.; Hao, Z.; Zhu, X.; Avci, U.; Miller, J.S.; et al. An *Arabidopsis* Cell Wall Proteoglycan Consists of Pectin and Arabinoxylan Covalently Linked to an Arabinogalactan Protein. *Plant Cell* **2013**, *25*, 270–287. [CrossRef]
55. Showalter, A.M. Arabinogalactan-proteins: Structure, expression and function. *Cell Mol. Life Sci.* **2001**, *58*, 1399–1417. [CrossRef]
56. Kong, Y.; Zhou, G.; Yin, Y.; Xu, Y.; Pattathil, S.; Hahn, M.G. Molecular Analysis of a Family of *Arabidopsis* Genes Related to Galacturonosyltransferases. *Plant Physiol.* **2011**, *155*, 1791–1805. [CrossRef]
57. Philippe, F.; Pelloux, J.; Rayon, C. Plant pectin acetylesterase structure and function: New insights from bioinformatic analysis. *BMC Genom.* **2017**, *18*, 456. [CrossRef]
58. Van Acker, R.; Déjardin, A.; Desmet, S.; Hoengenaert, L.; Vanholme, R.; Morreel, K.; Laurans, F.; Kim, H.; Santoro, N.; Foster, C.; et al. Different Routes for Conifer- and Sinapaldehyde and Higher Saccharification upon Deficiency in the Dehydrogenase CAD1. *Plant Physiol.* **2017**, *175*, 1018–1039. [CrossRef]
59. Bonawitz, N.D.; Chapple, C. The Genetics of Lignin Biosynthesis: Connecting Genotype to Phenotype. *Annu. Rev. Genet.* **2010**, *44*, 337–363. [CrossRef]
60. Irish, B.M.; Correll, J.C.; Koike, S.T.; Morelock, T.E. Three New Races of the Spinach Downy Mildew Pathogen Identified by a Modified Set of Spinach Differentials. *Plant Dis.* **2007**, *91*, 1392–1396. [CrossRef]